

Rotational spectroscopy, dipole moment and ^{14}N nuclear hyperfine structure of *iso*-propyl cyanide[☆]

Holger S.P. Müller^{a,*}, Audrey Coutens^{b,c}, Adam Walters^{b,c}, Jens-Uwe Grabow^d, Stephan Schlemmer^a

^a*I. Physikalisches Institut, Universität zu Köln, Zùlpicher Str. 77, 50937 Köln, Germany*

^b*Université de Toulouse; UPS-OMP; IRAP; Toulouse, France*

^c*CNRS; IRAP; 9 Av. colonel Roche, BP 44346, 31028 Toulouse cedex 4, France*

^d*Institut für Physikalische Chemie & Elektrochemie, Lehrgebiet A, Gottfried-Wilhelm-Leibniz-Universität, Callinstr. 3A, 30167 Hannover, Germany.*

Abstract

Rotational transitions of *iso*-propyl cyanide, $(\text{CH}_3)_2\text{CHCN}$, also known as *iso*-butyronitrile, were recorded using long-path absorption spectroscopy in selected regions between 37 and 600 GHz. Further measurements were carried out between 6 and 20 GHz employing Fourier transform microwave (FTMW) spectroscopy on a pulsed molecular supersonic jet. The observed transitions reach J and K_a quantum numbers of 103 and 59, respectively, and yield accurate rotational constants as well as distortion parameters up to eighth order. The ^{14}N nuclear hyperfine splitting was resolved in particular by FTMW spectroscopy yielding spin-rotation parameters as well as very accurate quadrupole coupling terms. In addition, Stark effect measurements were carried out in the microwave region to obtain a largely revised c -dipole moment component and to improve the a -component. The hyperfine coupling and dipole moment values are compared with values for related molecules both from experiment and from quantum chemical calculations.

Keywords:

rotational spectroscopy, dipole moment, hyperfine structure, nuclear quadrupole coupling, interstellar molecule

1. Introduction

Molecules containing the cyanide group, $-\text{CN}$, are quite numerous in space. Among the approximately 160 molecules detected in the interstellar medium or in circumstellar shells of late-type stars there are almost 30 molecules containing a cyano group, see for example the Molecules in Space web page¹ of the Cologne Database for Molecular Spectroscopy, CDMS [1, 2]. These include small inorganic species such as SiCN , cyanopolyynes HC_{2n-1}N up to HC_{11}N , as well as radicals and anions derived from the shorter cyanopolyynes. Saturated cyanides have been detected as well. Methyl cyanide, CH_3CN was among the earliest molecules to be detected in space by means of radio astronomy [3]. Transitions of rarer isotopologs, including CH_2DCN [4], have also been recorded. The heavier ethyl cyanide, $\text{C}_2\text{H}_5\text{CN}$, was detected in space more than 30 years ago [5], and isotopologs containing ^{13}C have been identified in Orion KL [6] and in Sagittarius B2(N) (Sgr B2(N) for short), where also corresponding isotopic species of vinyl cyanide were detected [7]. The latter two reports result from molecular line surveys of these two intensely studied high-mass

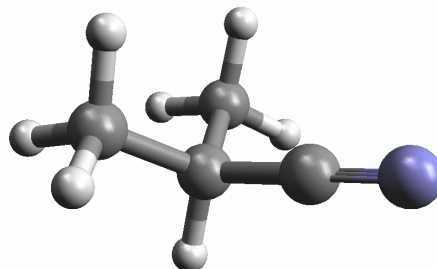


Figure 1: Schematic depiction of the molecular structure of *iso*-propyl cyanide.

star-forming regions carried out with the IRAM 30 m radio telescope on the Pico del Veleta near Granada, Spain in order to investigate the molecular complexities of these two prolific sources.

A part of the Sgr B2(N) region is called Large Molecule Heimat because many of the larger molecules have been detected there for the first time. In fact, the molecular line survey mentioned above, has revealed to date three new large molecules. The first one, aminoacetonitrile [8], is proposed to be the precursor for glycine, the simplest amino acid, a molecule awaiting its detection by radio-astronomy. The two others ones are ethyl formate and *n*-propyl cyanide, $n\text{-C}_3\text{H}_7\text{CN}$ [9]; the latter being the next larger member in the series of alkyl cyanides.

[☆]We dedicate this work to A. Robert W. McKellar, to Philip R. Bunker, and also to James K.G. Watson, who chose not to be officially named in this special issue, for their extensive contributions to experimental and theoretical molecular spectroscopy.

*Corresponding author.

Email address: hspm@ph1.uni-koeln.de (Holger S.P. Müller)

¹Internet address: <http://www.astro.uni-koeln.de/cdms/molecules>

Propyl cyanide, also known as butyronitrile, is the first alkyl cyanide which may occur in more than one isomeric form. The cyano group is attached to the first carbon atom of the propyl group in the *n*- or *normal*-form, thus yielding an unbranched chain, whereas it is attached to the second C-atom in *iso*-propyl cyanide, yielding a branched structure, as shown in Fig. 1. After the detection of *n*-propyl cyanide in space it was logical to look into the ratio between the chain isomer and the branched isomer of propyl cyanide which should provide insight into the astrochemistry of complex molecules.

There had been only two published investigations into the rotational spectrum of *iso*-propyl cyanide. Herberich [10] recorded more than 50 rotational, mostly *Q*-branch, transitions between 5 and 30 GHz with the *J* quantum numbers up to 57, but published only 22 with $J \leq 14$ and $K_a \leq 5$. The *a*-type spectrum was expected to be about 20 times stronger than the *c*-type spectrum, i.e. $|\mu_a/\mu_c| \approx 4.5$. The observations seemed to be in accord with these expectations, and, consequently, most of the published lines were *a*-types. Uncertainties were not stated, but seem to be much better than 100 kHz, possibly as low as 20 kHz for some of them. Quite accurate ^{14}N nuclear quadrupole coupling parameters were obtained from splitting observed in some transitions. No centrifugal distortion analysis was performed, but rotational constants were given.

Durig and Li [11] presented 10 *R*-branch transition frequencies obtained between 28 and 38 GHz along with 8 transition frequencies each for the three lowest vibrational states. The accuracies were estimated to be 0.2 MHz. They performed some structural evaluations and determined the dipole moment components from Stark effect measurements of three $J = 3 - 2$ *a*-type transitions with $K_a \leq 1$ as $|\mu_a| = 4.05 \pm 0.02$ D and $|\mu_c| = 1.4 \pm 0.2$ D. Neither work resolved possible splitting caused by internal rotation of the methyl groups.

A combined fit of these two data sets permitted some centrifugal distortion parameters to be determined, but the resulting predictions were not accurate enough to search for the molecule in the 3 mm region of the spectral survey of Sgr B2(N), the lowest frequency region that was also deemed to be the best to search for such complex molecules. Therefore, an extensive laboratory study has been initiated to record rotational transitions in selected frequency windows from the microwave to the submillimeter region to obtain very accurate rotational and centrifugal distortion parameters as well as greatly improved ^{14}N hyperfine (hf) coupling values. Noting that the *c*-type transitions appeared to be much weaker than predicted from the published dipole moment components, we also carried out Stark effect measurements which have resulted in large improvement for both components and yielded a much smaller value for the *c*-component.

2. Experimental details

Absorption spectra of *iso*-propyl cyanide in the millimeter (mm) and submillimeter (sub-mm) regions were recorded at the Universität zu Köln. The 37 – 69 GHz range was covered with a commercial synthesizer (Agilent E8257D) as source, which nominally extends from almost 0 to 67 GHz. Its output was

amplified and frequency-stabilized by a phase-lock loop (PLL) referenced to a rubidium reference. The lower frequency cut-off was caused by the amplifier. A Schottky-diode was used as detector. The amplified output of the same synthesizer was used to drive a commercial frequency quadrupler (VDI-AMC-S150e) and a superlattice frequency multiplier [12] in series for investigations between 303 and 346 GHz. Additional measurements were performed in the frequency range 589–600 GHz with the Cologne Terahertz Spectrometer [13] using a phase-locked backward-wave oscillator as source. A liquid He-cooled InSb hot-electron bolometer was used as detector in the sub-mm region. To increase the sensitivity, frequency-modulation was employed throughout. Demodulation at twice the frequency causes a line-shape which is close to the second derivative of a Gaussian.

A 6 m long absorption cell was used in the lower two frequency regions while a 3 m long cell was employed near 600 GHz. A commercial sample of *iso*-propyl cyanide (Sigma-Aldrich) was used without further purification at pressures of around 0.1 Pa to around 1 Pa. All measurements were carried out at room temperature.

Spectra of *i*-C₃H₇CN between 6.8 and 19.9 GHz were recorded at the Gottfried-Wilhelm-Leibniz-Universität in Hannover using a supersonic-jet Fourier transform microwave (FTMW) spectrometer [14] in the coaxially oriented beam-resonator arrangement (COBRA) [15] using a very broadband (2–26.5 GHz) and very sensitive set-up [16, 17]. The sample was highly diluted with Ne to a total pressure of 100 kPa and expanded through a solenoid valve (General Valve series 9, nozzle orifice diameter 1.2 mm) into the Fabry-Pérot type resonator. A repetition rate of 20 Hz was used for the pulsed expansion. Following transient absorption, the spectral positions of the MW transient emission were determined after Fourier transformation of the 4k-data-point time-domain signal recorded at intervals of 100 ns, being 4k-zero-padded prior to transformation. Each molecular signal is split by the Doppler effect as a result of the coaxial arrangement of the supersonic jet and resonator axes in the COBRA set-up. The rest frequencies are calculated as the arithmetic mean of the frequencies of the two Doppler components. The accuracies range from 0.3 to 0.5 kHz because of the very high signal-to-noise ratio and very favorable, symmetric line shapes.

Stark effect measurements were performed with the same spectrometer employing the coaxially aligned electrodes for Stark-effect applied in resonators (CAESAR) setup [18], which provides a fairly homogeneous electric field over the entire volume, from which molecules are effectively contributing to the emission signal.

3. Quantum chemical calculations

The commercially available program Gaussian 03 [19] was used mainly to calculate the ^{14}N nuclear quadrupole tensors for *iso*-propyl cyanide and two related molecules in their inertial and principal axes systems and also to compare other experimental spectroscopic parameters with quantum-chemically evaluated ones. The popular hybrid density-functional theory

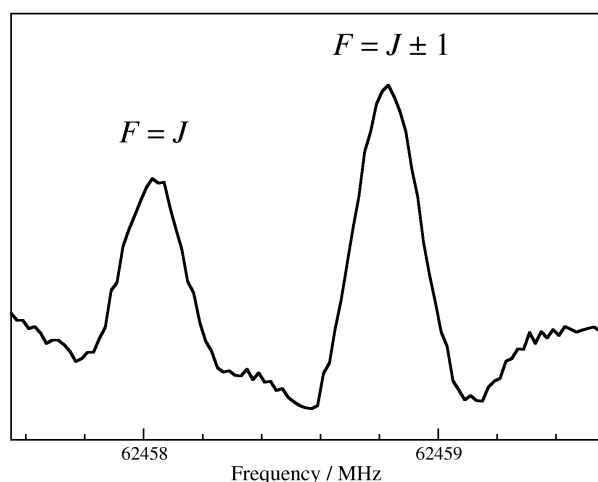


Figure 2: The prolate paired $J_{K_a} = 9_8 - 8_8$ transitions of *iso*-propyl cyanide in the millimeter region showing partially resolved ^{14}N hyperfine (hf) splitting; the F quantum numbers are given. Prolate paired transitions are those for which the two transitions involving levels with $K_c = J + K_a$ and $K_c = J + K_a + 1$ are not resolved; the K_c quantum numbers are frequently omitted in these cases. The role of K_a and K_c is reversed in oblate paired transitions.

method B3LYP and the MP2 method were used. The correlation consistent basis set aug-cc-pVTZ of triple zeta quality was used for tight convergence structure calculations and for harmonic force field calculations which also yield equilibrium quartic centrifugal distortion parameters. As the program usually does not put molecules into the inertial axis system, the molecules were rotated accordingly, and dipole moments and hyperfine parameters were evaluated requesting no symmetry to be used. Core-correlating basis functions were included for the latter calculations to arrive at the aug-cc-pwCvTZ basis set [20]. The MP2 density was requested for the corresponding calculations, as this was not the default. These calculations were performed with the core electrons frozen, which is the default. Trial calculations of the nuclear quadrupole properties at the MP3 level without structure optimization turned out to be barely justifiable in terms of required time and results. These calculations were done at the MP2/aug-cc-pVTZ structures. Corresponding calculations with structure optimization or even higher level calculations were deemed to be too time-consuming. Finally, the nuclear spin-rotation parameters (requesting output=Pickett) are provided defined negatively which is in accord with the NMR conventions and with the initial spectroscopic conventions, but nowadays, they are given almost exclusively defined positively in spectroscopy.

4. Observed spectrum and analysis

The *iso*-propyl cyanide molecule is a rather asymmetric rotor of the prolate type ($\kappa = -0.5766$) with a large a -dipole moment component and a still sizable c -component as mentioned in section 1. Previous studies [10, 11] did not resolve any methyl internal rotation splitting. In fact, even the resolution attainable with FTMW spectroscopy (line widths of order of 3 kHz) did

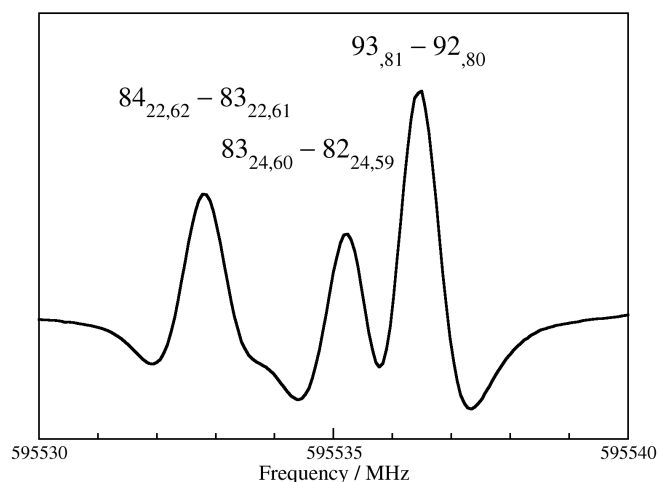


Figure 3: Detail of the sub-millimeter spectrum of *iso*-propyl cyanide showing two individual and one oblate paired transitions with the K_a quantum numbers for the latter being omitted; see also caption to Fig. 2.

not reveal any such splitting. The spin of the ^{14}N nucleus is 1, leading to nuclear quadrupole splitting, which at lower frequencies and high resolution can be resolved. The magnetic moment of this nucleus can modify the quadrupole splitting because of the nuclear spin-rotation coupling. However, for a molecule with such small rotational constants and for a nucleus with such small magnetic moment, such effects are expected to be very small. $I(^{14}\text{N}) = 1$ causes each rotational level to be split into three hf levels. The hf selection rules are $\Delta F = 0, \pm 1$. The strong components have $\Delta F = \Delta J$, but the weaker components can be observed under favorable conditions, in particular for low- J transitions. At somewhat higher quantum numbers, the $F = J \pm 1$ components may overlap while the one with $F = J$ may still be resolvable as shown in Fig. 2. Eventually no hf splitting can be resolved (e.g. Fig. 3) unless one resorts to sub-Doppler techniques.

Predictions from a combined fit of previous data were good enough to search for some lower- J quantum number a -type R -branch transitions in small frequency windows of the lower mm region (37 – 69 GHz). Pickett’s SPCAT and SPFIT programs [21] were used for prediction and fitting of the spectra, respectively. With refined predictions, transitions with higher J and K_a were recorded. Later, a -type Q -branch transitions, first with $\Delta K_a = 0$, subsequently with $\Delta K_a = 2$, were found together with very few unexpectedly weak c -type transitions. Even though the molecule has several low-lying vibrational modes, the spectrum was sparse enough in the lower millimeter region that overlap of transitions searched for occurred only on few occasions and mostly for rather weak transitions. Some of the transitions showed splitting caused by the ^{14}N nuclear hyperfine coupling as can be seen in Fig. 2. Unresolved asymmetry splitting occurred frequently for transitions having relatively high K_a and low J values (prolate pairing, shown in Fig. 2) or, at higher frequencies, for those with low K_a and high J values (oblate pairing, shown in Fig. 3).

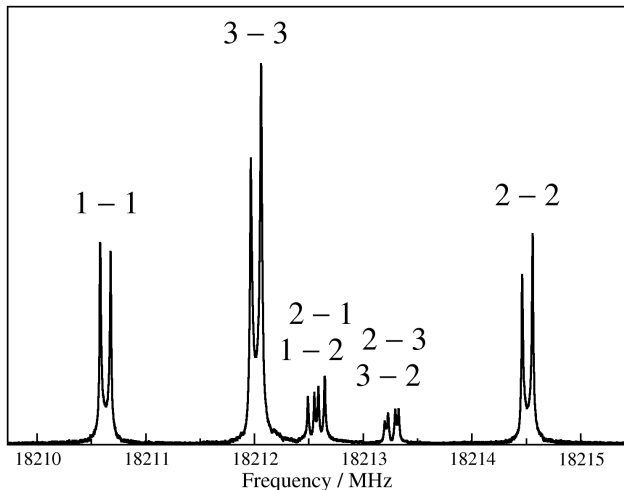


Figure 4: The $J_{K_a, K_c} = 2_{2,1} - 2_{0,2}$ transition of *iso*-propyl cyanide recorded in several sections by molecular beam Fourier transform microwave spectroscopy. The ^{14}N hf splitting is well resolved; the $F' - F''$ quantum numbers are given. Each line is split into two Doppler components because the microwave radiation propagates in the same direction as the supersonic jet. Because of the very high sensitivity, not only the three strong $\Delta F = 0$, but also the four weaker $\Delta F \neq 0$ hf components are seen.

Subsequently, measurements of selected transitions were performed in the lower (303 – 346 GHz) and somewhat higher sub-mm region (589 – 600 GHz). These were mostly *a*-type transitions, see Fig. 3, but also a considerable number of *c*-type transitions. Transitions having $\Delta K_a \geq 2$ were not searched for, except in one case, because they were rather weak, and the predicted uncertainties were usually smaller than those of *c*-type transitions of similar strengths. Quantum numbers J and K_a as high as 103 and 59, respectively, have been accessed.

The observation of the *c*-type transitions being much weaker than predicted from the published dipole moment components prompted new Stark effect measurements by FTMW spectroscopy as described in section 5. We used the opportunity to record some transitions in the absence of an electric field in order to improve the hyperfine parameters as well as the lower order spectroscopic parameters. The very high sensitivity of the spectrometer permitted to observe not only the strong $\Delta F = \Delta J$ hf components, but also the weaker ones, even for transitions already not so strong as is demonstrated in Fig. 4.

468 transitions belonging to slightly more than 300 distinct spectral features were used in the final fit. 41 hf components of 9 rotational transitions were obtained in the microwave region. Of the more than 100 transitions from the millimeter region almost half represent partially resolved hf features, some of which showed prolate pairing. More than 150 transitions each were recorded slightly above 300 and below 600 GHz, respectively; several of these are unresolved asymmetry doublets. The few previously reported transition frequencies were omitted from the final fit as their uncertainties were rather large in one case and rather uncertain in the other. Moreover, trial fits showed that omission of these data had a negligible effect on the values as well as the uncertainties of the spectroscopic pa-

Table 1: Experimentally determined spectroscopic parameters^a (MHz) of *iso*-propyl cyanide in comparison to those from quantum chemical calculations^b

Parameter	Experimental value	B3LYP	MP2
A	7940.877174 (31)	7934.0	8022.5
B	3968.087775 (27)	3974.1	3936.3
C	2901.053223 (22)	2899.0	2914.9
$D_K \times 10^3$	-5.23242 (61)	-4.50	-5.50
$D_{JK} \times 10^3$	12.17725 (42)	11.55	12.62
$D_J \times 10^6$	610.2684 (153)	593.	610.
$d_1 \times 10^6$	-244.0908 (69)	-240.	-239.
$d_2 \times 10^6$	-189.2889 (76)	-180.	-189.
$H_K \times 10^9$	-37.163 (248)		
$H_{KJ} \times 10^9$	10.968 (281)		
$H_{JK} \times 10^9$	38.267 (140)		
$H_J \times 10^{12}$	-584.83 (151)		
$h_1 \times 10^{12}$	68.73 (77)		
$h_2 \times 10^{12}$	884.23 (83)		
$h_3 \times 10^{12}$	322.39 (140)		
$L_{KKJ} \times 10^{15}$	-242. (61)		
$L_{JJK} \times 10^{15}$	-79.7 (95)		
$l_3 \times 10^{15}$	-1.658 (148)		
$l_4 \times 10^{15}$	-0.607 (41)		
χ_{aa}	-3.93838 (23)	-4.380	-3.584
χ_{bb}	2.11117 (30)	2.338	1.919
χ_{cc}	1.82721 (24) ^c	2.042	1.665
$C_{aa} \times 10^3$	0.162 (76)	0.2	0.1
$C_{bb} \times 10^3$	0.834 (97)	0.9	0.8
$C_{cc} \times 10^3$	0.583 (74)	0.6	0.5

^aNumbers in parentheses are one standard deviation in units of the least significant figures.

^bSee section 3 for details.

^cDerived parameter.

rameters.

Rotational constants along with complete sets of quartic and sextic as well as some octic centrifugal distortion parameters were determined employing Watson’s *S*-reduction of the rotational Hamiltonian. The *A*-reduction yielded a slightly worse result even with one parameter more in the fit. The highly accurate data obtained by FTMW spectroscopy not only permitted ^{14}N nuclear quadrupole coupling values to be evaluated, but also yielded nuclear spin-rotation coupling constants. Trial fits with the off-diagonal quadrupole term χ_{ac} yielded -1.06 ± 1.57 for its magnitude; the sign cannot be determined from the fit, but can often be deduced from the values of the diagonal terms. Even though this value appears to be reasonable, the parameter was omitted from the final fit as it was not even close to being determined with significance. In addition, inclusion of the parameter did have a negligible effect on the quality of the fit and on the values of all other parameters. The final spectroscopic parameters are given in Table 1 together with values from quantum chemical calculations as far as available. The rms error of the fit is 0.85 and differs little for subsets of the data (between 0.74 and 0.96), indicating essentially appropriate estimates of the uncertainties. The measured transition frequencies with their assignments, uncertainties, and residuals between observed values and those calculated from the final set of spectroscopic parameters are given in the supplementary material. Predictions of the rotational spectrum along with a documen-

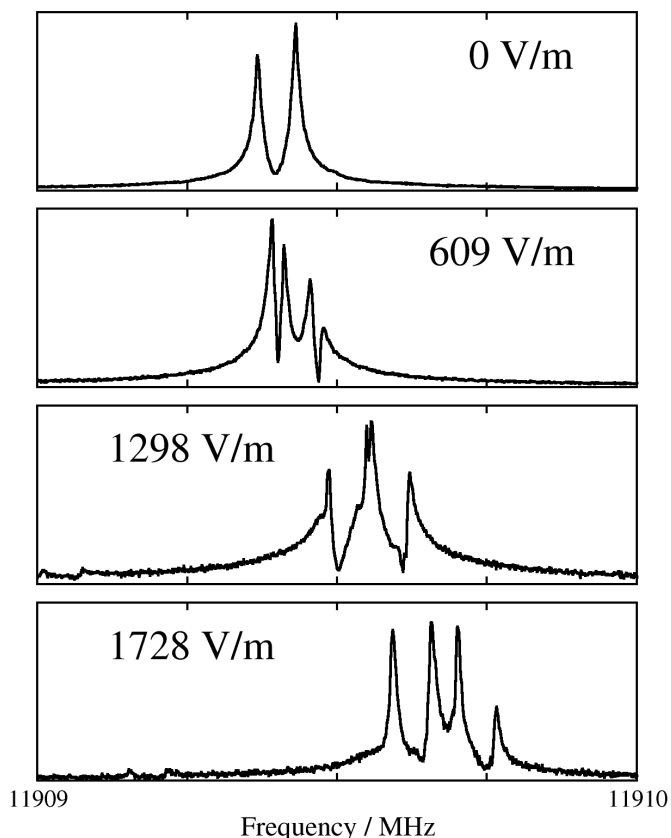


Figure 5: Stark effect measurements of the $F = 1 - 1$ hyperfine component pertaining to the $J_{K_a, K_c} = 1_{1,0} - 0_{0,0}$ transition of *iso*-propyl cyanide. Each molecular signal is split into two because of the Doppler effect; see also caption to Fig. 4. The hf component splits into two m -components upon application of a static electric field because of the $\Delta M = \pm 1$ selection rules. The electric field increases almost linearly from top to bottom, and the frequency shifts display the second order or quadratic Stark effect.

tation will be provided in the catalog section² of the Cologne Database for Molecular Spectroscopy, CDMS [1, 2]. Line, parameter, and fit files, along with further auxiliary files, will be available in the data section³ of the CDMS, and can also be accessed via the archive part of the catalog.

5. Stark effect measurements

The Stark field is perpendicular to the polarization of the microwave field leading to the selection rules $\Delta M = \pm 1$ [18]. Transitions with small J quantum numbers are frequently used for determining dipole moment components as these usually display large quadratic Stark shifts. In the present case, with hf splitting caused by the ^{14}N nucleus, the $F' - F'' = 1 - 0$ (or $0 - 1$) and the $1 - 1$ components were deemed to be particularly suited for Stark effect measurements as these would lead to only one and two Stark components, respectively, thus minimizing the danger of line overlap. Fig. 5 demonstrates the

second order Stark effect for one $1 - 1$ hf component which splits into two Stark components. Table 2 summarizes the chosen transitions, hf, and Stark components as well as results from the analysis of the Stark effect. Other hf components were less suitable because of overlap already in the absence of an electric field or because overlap occurred at rather low fields, both making frequency determinations less reliable.

The voltage readings were corrected marginally as described in ref. [22]. The distance calibration was also taken from that work; however, it was noticed that the dipole moment used for OC^{36}S was actually that of the main isotopolog involving ^{32}S . The dipole moment of OC^{36}S has, to our knowledge, not been determined experimentally, but its value can be evaluated by applying the $\text{OC}^{34}\text{S}/\text{OC}^{32}\text{S}$ dipole ratio to OC^{34}S . We used the case (1) model data from ref. [23] to derive a value of 0.71564 D with an estimated uncertainty of about 0.05 mD.

The analysis was carried out with the program QSTARK [24]. Most of the Stark-shifted frequencies were given unit weight, some, associated with lines displaying higher noise or less favorable lineshapes were given slightly lower weights. Measurements with two Stark components very close to each other were not used in the fit as the frequencies were rather uncertain. Only the two non-zero dipole moment components μ_a and μ_c were allowed to vary in the fit. The statistical error was only 1.6 mD for μ_a , a relative uncertainty of 4×10^{-4} . Thus, other sources of error should be considered. The limitations of determining the accuracies of the voltages should be included in the statistical uncertainties as very many Stark-shifts have been measured, thus, they should behave like statistical errors. The uncertainty in the constant voltage off-set should also matter little because it is not linearly dependent on the voltage. The neglect of the isotope dependence of the OCS dipole moment would have created a non-negligible error of 6.3×10^{-4} , but the individual OCS dipole moments have been determined to better than 10^{-4} . Also, the uncertainty in the linear voltage correction is comparatively small (1.5×10^{-4}). However, the two plate separations have uncertainties of about 5 and 9×10^{-4} , respectively, which both exceed the purely statistical error. The final uncertainty of μ_a has been increased to 5.0 mD, which is slightly larger than the maximum error of the plate separation combined with the statistical error. Table 2 summarizes the Stark effect measurements while Table 3 displays the experimental and theoretical dipole moment values for *iso*-propyl cyanide from this study together with values for two related molecules.

6. Discussion

Accurate spectroscopic parameters have been determined for *iso*-propyl cyanide in the course of the present investigation. The rotational constants are consistent with the less accurate ones from previous studies [10, 11], in particular taking into account that these studies did not perform centrifugal distortion analyses. As can be seen in Table 1, the experimental rotational and quartic centrifugal distortion parameters agree favorably with the theoretical values, in particular if one considers that, first, the latter are equilibrium values, while the former are ground-state values, and second, the models are of limited

²Internet address: <http://www.astro.uni-koeln.de/cdms/catalog>

³Internet address: <http://www.astro.uni-koeln.de/cdms/daten>

Table 2: Stark effect measurement of *iso*-propyl cyanide giving first the quantum numbers of the rotational transition, the hyperfine structure component, and the Stark component, and subsequently the applied electric fields (V/m), the measured frequencies (MHz), the weights of the measurement in the fit, and the residuals O-C (kHz)

$J'_{K'_a K'_c} - J''_{K''_a K''_c}, F' - F'', M'_F - M''_F$	Field	Frequency	Weight	O-C
$1_{01} - 0_{00}, 1 - 1, 0 - 1$				
	0.0	6868.15324	1.00	-0.12
	1280.5	6868.17406	0.25	-1.36
	1705.0	6868.19216	0.25	-0.30
	2299.5	6868.22285	0.25	-1.63
$1_{01} - 0_{00}, 1 - 1, 1 - 0$				
	0.0	6868.15324	1.00	-0.12
	1280.5	6868.18955	0.25	-0.80
	1705.0	6868.21706	0.25	-1.61
	2299.5	6868.27052	0.25	-0.72
$1_{01} - 0_{00}, 0 - 1, 0 - 1$				
	0.0	6871.10657	1.00	0.14
	431.5	6871.11008	1.00	0.00
	601.0	6871.11354	1.00	0.03
	856.0	6871.12041	1.00	-0.40
	1280.5	6871.13795	0.44	-0.72
	1705.5	6871.16281	0.25	-0.98
$1_{10} - 0_{00}, 0 - 1, 0 - 1$				
	0.0	11908.02845	1.00	0.54
	437.0	11908.04335	1.00	0.35
	609.0	11908.05792	1.00	0.87
	867.5	11908.08663	1.00	0.35
	1298.0	11908.15459	1.00	0.36
	1728.5	11908.23989	1.00	-0.70
$1_{10} - 0_{00}, 1 - 1, 1 - 0$				
	0.0	11909.39865	1.00	0.03
	867.5	11909.44876	1.00	0.09
	1298.0	11909.51770	1.00	0.51
	1728.5	11909.62373	1.00	0.02
$1_{10} - 0_{00}, 1 - 1, 0 - 1$				
	0.0	11909.39865	1.00	0.03
	867.5	11909.48263	1.00	-0.05
	1298.0	11909.58742	1.00	0.63
	1728.5	11909.73230	1.00	0.03
$2_{12} - 1_{11}, 1 - 0, 1 - 0$				
	0.0	12672.69853	1.00	-0.18
	434.0	12672.71000	1.00	0.17
	605.5	12672.72030	1.00	-0.19
	862.0	12672.74265	1.00	-0.77
	1289.5	12672.80158	1.00	-0.15
	1717.5	12672.88826	1.00	0.07
$2_{11} - 1_{10}, 1 - 0, 1 - 0$				
	0.0	14806.68033	1.00	-0.60
	435.5	14806.67043	1.00	-0.91
	607.0	14806.66176	1.00	-0.71
	864.5	14806.64461	1.00	0.36
	1293.0	14806.60375	1.00	0.57
	1722.0	14806.55352	1.00	-0.73
$2_{11} - 1_{01}, 1 - 0, 1 - 0$				
	0.0	19843.60228	1.00	-0.13
	434.0	19843.60374	1.00	-0.34
	604.5	19843.60560	1.00	-0.05
	861.5	19843.60905	1.00	0.06
	1289.0	19843.61691	1.00	-0.19
	1716.5	19843.62793	1.00	-0.44
	2315.0	19843.64930	1.00	0.00
	2742.5	19843.66830	1.00	0.52
	3255.0	19843.69289	1.00	-0.72

sophistication. The very good agreement between the experimental and the B3LYP rotational constants compared to those obtained at the MP2 level may be fortuitous, though. In the case of a molecule close to the prolate limit, D_K is usually positive and shows a fairly strong variation with vibrational excitation, as can be seen for the chlorine dioxide molecule [27]. In the present case, D_K is negative and smaller in magnitude than D_{JK} . The somewhat larger deviation between experimental and B3LYP D_K values of *iso*-propyl cyanide, compared with the remaining quartics, may well be explained by unaccounted vibrational effects. The very good agreement between some of the experimental and MP2 quartics is probably fortuitous.

The previously determined ^{14}N nuclear quadrupole coupling parameters [10] are in quite good accord with the present, more accurate ones in Table 1. The agreement with quantum-chemically calculated ones, also in that table, are reasonable. Again, the deviations may be due to vibrational effects and to short-comings of the theoretical methods. The magnitudes of the MP2 values are smaller than the experimental values by about the same amount as the B3LYP magnitudes are too large. Vibrational corrections to nuclear quadrupole coupling values are often very small, as in HC_3N and DC_3N [28], to moderate (a few percent), as in DCO^+ [29], H_2^{17}O [30], and D_2O [31]. Thus, one would attribute the deviations between theoretical and experimental values of around 10 % more to deficiencies of the quantum chemical methods than to vibrational effects, at least in one of the two methods. It should be noted, though, that large vibrational effects ($\sim 15\%$) are present in the ^{14}N quadrupole coupling constant of HN^{13}C [29] caused mainly by the floppy bending mode.

Assuming the main principal axis of a nuclear quadrupole tensor to be aligned with a respective bond can lead to large errors in the derived principal values. An extreme case has been resolved by diagonalizing the ^{35}Cl quadrupole tensor of SOCl_2 free of assumptions [32]. The value of χ_z was smaller by about one third and more compared to previous MW studies and very little π -bonding had to be inferred, in line with expectations, and with nuclear quadrupole resonance measurements, but in contrast to previous microwave results. A similar effect may occur if the main principal axis of the quadrupole tensor is in fact aligned with a respective bond, but the angles of this bond to the inertial axes are not known sufficiently well. There does not seem to be any electron diffraction study available for *iso*-propyl cyanide. Hence, the only experimental structural data available seem to be those from the more recent previous microwave study [11]. Not knowing how reasonable these are, it was decided to perform quantum chemical calculations for further insight into the quadrupole coupling of *iso*-propyl cyanide and two related molecules. The results have been summarized in Table 4.

The quadrupolar z -axis is tilted away from the CN bond by very small amounts for all three molecules as one would have expected. There are (at least) three options for diagonalizing the ^{14}N nuclear quadrupole tensor: first, one could start from the calculated θ_{za} angle, second, one could start from the calculated $\eta = (\chi_x - \chi_y)/\chi_z$ value, and finally, one could scale the calculated χ_{ac} value with the ratio of the observed and calculated

Table 3: Experimental dipole moment components (D) of *iso*-propyl cyanide in comparison to values from quantum-chemical calculation and corresponding values for the *anti*-conformer of *normal*-propyl cyanide and for *cyclo*-propyl cyanide^a

Component	<i>i</i> -Propyl cyanide			<i>a-n</i> -Propyl cyanide			<i>c</i> -Propyl cyanide		
	Exptl.	B3LYP	MP2	Exptl. ^b	B3LYP	MP2	Exptl. ^c	B3LYP	MP2
μ_a	4.0219 (50)	4.119	3.991	3.597 (59)	4.150	4.021	4.1221 (31)	4.317	4.151
$\mu_{b/c}$ ^d	0.6192 (267)	0.707	0.702	0.984 (15)	1.095	1.080	0.9026 (9)	0.911	0.915
μ_{tot}	4.0693 (275)	4.179	4.052	3.729 (58)	4.292	4.164	4.2197 (30)	4.413	4.251

^aSee section 3 for details on quantum chemical calculations. Numbers in parentheses are one standard deviation in units of the least significant figures.

^bRef. [25].

^cRef. [26].

^d*c*-Component for *iso*- and *cyclo*-propyl cyanide; *b*-component for the *anti*-conformer of *normal*-propyl cyanide.

Table 4: Experimental ¹⁴N nuclear quadrupole coupling parameters χ_{ii} (MHz) of *iso*-propyl cyanide estimated^a off-diagonal coupling term χ_{ij} (MHz), angle (deg) between quadrupolar *z*-axis and the CN bond, and derived principal coupling value χ_z (MHz) and η^b (unitless) in comparison to values from quantum-chemical calculations^c and corresponding values for the *anti*-conformer of *normal*-propyl cyanide and for *cyclo*-propyl cyanide

Parameter	<i>i</i> -Propyl cyanide				<i>a-n</i> -Propyl cyanide				<i>c</i> -Propyl cyanide			
	Exptl.	B3LYP	MP2	MP3	Exptl. ^d	B3LYP	MP2	MP3	Exptl. ^e	B3LYP	MP2	MP3
χ_{aa}	-3.938	-4.380	-3.584	-3.969	-3.440	-3.843	-3.117	-3.476	-3.460	-3.867	-3.123	-3.473
χ_{bb}	2.111	2.338	1.919	2.120	1.385	1.560	1.227	1.385	1.746	1.895	1.643	1.717
χ_{cc}	1.827	2.042	1.665	1.849	2.056	2.283	1.890	2.092	1.714	1.972	1.480	1.756
χ_{ax}^f	-1.278	-1.416	-1.218	-1.338	-2.057	-2.285	-1.895	-2.103	-2.013	-2.186	-1.801	-2.041
$\angle(z, \text{CN})$	—	0.16	0.27	—	—	0.24	0.39	—	—	-0.04	0.16	—
χ_z	-4.209	-4.679	-3.853	-4.262	-4.198	-4.679	-3.827	-4.260	-4.151	-4.595	-3.744	-4.175
η	0.003	-0.001	-0.004	-0.001	-0.021	-0.024	-0.012	-0.018	-0.170	-0.175	-0.122	-0.178

^aThe B3LYP value was scaled with the χ_{kk} ratio of the experimental and B3LYP value; see section 6 for details.

^b $\eta = (\chi_x - \chi_y)/\chi_z$.

^cSee section 3 for details on quantum chemical calculations. Numbers in parentheses are one standard deviation in units of the least significant figures.

^dRef. [33]; uncertainties of the experimental χ_{ii} are in the last digit.

^eRef. [26]; uncertainties of the experimental χ_{ii} are in the last digit.

^f $x = c$ for *iso*- and *cyclo*-propyl cyanide; $x = b$ for the *anti*-conformer of *normal*-propyl cyanide.

χ_{bb} values; in the case of *n*-propyl cyanide, it would be χ_{ab} and χ_{cc} , respectively. Ideally, each option should lead to the same result. In practice, the B3LYP values lead to slightly different estimates for the experimental χ_{ac} value: -1.271, -1.317, and -1.278, respectively. The magnitudes of these values are close to the 1.06 MHz determinable from the fit, see section 4; but since the uncertainty of the latter is larger than its value, this agreement is not very meaningful. The values for η differed slightly more, those for χ_z differed slightly less. The latter option was chosen since it resulted in magnitudes for the non-zero off-diagonal quadrupole coupling constant and the χ_z value that were between the other two. Trial fits employing the *cyclo*-propyl cyanide data set [26] revealed that $\chi_{ac} \approx 2.8$ can be obtained, albeit barely with significance if the stated uncertainties of 2 kHz for the FTMW data are used. These uncertainties seem conservative given an achievable rms value of 0.64 kHz and a data set of as many as 48 different FTMW lines.

Nuclear quadrupole coupling parameters calculated at the MP3/aug-cc-pwCVTZ level were much closer to experimental values for all three molecules than values calculated at the MP2 or B3LYP levels. This may be seen as an indication that vibrational effects on the quadrupole parameters are possibly rather small for all these molecules. However, the agreement may as well be fortuitous as the level may be still too low. These parameters were calculated at the structural parameters optimized at the MP2/aug-cc-pVTZ level because of computational time constraints, not at a structure optimized at the MP3 level. This will only have a sufficiently small effect if the structural parameters calculated at the MP3 level are sufficiently close to those

at the MP2 level.

It is noteworthy that Durig and Li estimated values $\chi_{ac} = -1.22$ MHz and $\chi_z = -4.15$ MHz by assuming the *z*-axis to be aligned with the CN bond. These values are remarkably close to the present values in Table 4, suggesting that their preferred structural parameters are reasonable. They also deduced $\eta \approx 0$.

The χ_z values, reported in Table 4, are also very similar among the three related molecules *iso*- and *cyclo*-propyl cyanide and the *anti*-conformer of *normal*-propyl cyanide in Table 4, and the small differences with respect to *cyclo*-propyl cyanide are probably significant. In fact, values very close to -4.2 MHz have been determined for a variety of organic cyanides: ~ -4.14 MHz for ethyl cyanide [34], -4.22 MHz for methyl cyanide [35, 36], ~ -4.27 or ~ -4.18 MHz for vinyl cyanide [37, 38], -4.237 for phenyl cyanide [39], and even values for HC₃N and DC₃N, -4.3192 and -4.318 MHz, respectively [40, 28], are not very different. The situation for cyanoketene, $\chi_z \approx -3.94$ MHz [41], is uncertain not only because of the large error bar, but also because small deviations from the assumed position of the *z*-axis may have a substantial effect on the χ_x and χ_z values because the CN bond is bent far away from all axes. Cyanocyclopropenyldiene, in which the *z*-axis essentially agrees with the *a*-axis, and thus $\chi_z = -4.495$ MHz [42], and hydrogen cyanide, $\chi_z = -4.7078$ MHz [43], have larger values. Similarly, a value of -4.61 MHz has been inferred for acetyl cyanide aided by quantum chemical calculations [44].

The value of η is a measure of the deviation of the principal nuclear quadrupole tensor from cylindrical symmetry. If the nu-

cleus belongs to an atom that is located in a terminal position of a formal single bond, η is interpreted as a measure of the π -character, and hence the double bond character of that single bond. The CN bond, however, is probably as close to a true triple bond as is possible between two main group elements. Hence, η is certainly not a direct measure of the π -character of that bond. It can, instead, be viewed as an indication, how much the triple bond character has been decreased. The magnitude of η should be very small for a primary alkyl cyanide and increase somewhat for secondary and tertiary alkyl cyanides. Further increase should occur if the cyano group is attached to a small saturated ring molecule, and even more so, if it is attached to an atom which is involved in π -bonding. As can be seen in Table 4, η is close to zero for the *anti*-conformer of *normal*-propyl cyanide. However, it is much closer to zero for *iso*-propyl cyanide, and it is zero because of symmetry in *tertiary*-butyl cyanide. The nuclear quadrupole tensor in its principal axis system deviates considerably for *cyclo*-propyl cyanide, and it is not so common that a diagonal quadrupole tensor in its inertial axis system is more symmetric than in its principal axis system. On the other hand, η is quite close to zero in vinyl cyanide [37, 38], suggesting that there is little interaction between the π -electrons of the vinyl group and those of the cyano group. Together with the very similar values for χ_z , this suggests that the CN group in all these molecules has a triple bond. Thus, it cannot be surprising that for all three investigated conformers of *n*-butyl cyanide good agreement with experimentally measured quadrupole coupling parameters was obtained when the cylindrically symmetric quadrupole tensor of methyl cyanide was rotated into the corresponding inertial axis systems [45]. This bonding model appears to be a good approximation even for phenyl cyanide, since $\eta = -0.080$ [39] is also fairly close to zero. The principal quadrupole tensors of acetyl cyanide, cyanoketene, and cyanocyclopropenylidene display larger deviations from cylindrical symmetry with η values of about 0.19 [44], -0.37 [41], and 0.38 [42], respectively. As mentioned above, the value of cyanoketene is somewhat more uncertain. A factor of $1/4$ for $\chi_{bb} - \chi_{cc}$ of cyanopropenylidene has been forgotten in the publication [42]. Finally, a value of $\eta \approx 0.2$ was found as typical for cyano groups attached to carbonyl groups [44], based on several examples.

It may, at first sight, be surprising that nuclear magnetic spin-rotation parameters can be determined with some accuracy for a nucleus having a small magnetic g -factor and being in a molecule with comparatively small rotational constants. Comparison between experimental and theoretically calculated values in Table 1 are favorable given the available accuracies. ^{14}N spin-rotation parameters with very similar values can be determined for the related *cyclo*-propyl cyanide employing the published data set [26]. Such parameters have been determined from FTMW spectroscopy and published, e.g., for the slightly lighter vinyl cyanide [7, 38] or the fairly heavy SOCl_2 [32].

As can be seen in Table 3, a very accurate μ_a value of 4.0219 (50) D has been determined for *iso*-propyl cyanide, its accuracy is mainly limited by the calibration uncertainties as mentioned in section 5. The previously determined value of 4.05 (2) D [11] is essentially the same, only its uncertainty

is somewhat larger. The c -component was determined here as 0.6192 (267) D. The uncertainty is much larger than that of the a -component because all Stark-shifts are dominated by the latter component. This value does not agree at all with 1.4 (2) D determined in an earlier study [11]. This large difference results in a factor of 5 weaker line intensities. In fact, the average line intensity ratio between a and c -type transitions is 42, about a factor of two more than was estimated in Ref. [10].

The experimental dipole moment components of *iso*- as well as *cyclo*-propyl cyanide agree rather well with those from quantum-chemical calculations which are all presented in Table 3. This is not the case for the *anti*-conformer of *n*-propyl cyanide. Assuming deviations to be similar to those observed for the other two molecules, one would expect $\mu_a \approx 4.0$ D instead of ~ 3.6 D from experiment [25]. It may be warranted to revisit the Stark effect measurements of *n*-propyl cyanide. The experimental and theoretical values for μ_b , on the other hand, are in accord. It may be noted that in *iso*-propyl cyanide the angle of the dipole vector with the a -axis is quite similar to the angle between the CN bond and the a -axis, the latter is only 2.3° bent farther away, but this is an exception. For both *cyclo*-propyl cyanide as well as the *anti*-conformer of *n*-propyl cyanide, the CN bond is bent farther away from the a -axis as well as from the dipole vector.

Irrespective of the controversy concerning the size of the b -dipole moment component of ethyl cyanide [46], its total dipole moment is about 4.05 D, marginally larger than 3.922 D of methyl cyanide [47], and also close to ~ 3.9 D of vinyl cyanide [37], showing little variation among monocyanides of saturated or almost saturated hydrocarbons.

7. Conclusions

The rotational spectrum of *iso*-propyl cyanide has been investigated from the MW well into the sub-mm region at 600 GHz. Accurate rotational constants as well as centrifugal distortion parameters have been obtained. These are sufficiently accurate to search for the molecule in space in all regions relevant for radio-astronomy. The isomer *n*-propyl cyanide was detected in the prolific Galactic center hot-core source Sgr B2(N) in the course of a line survey which covered the entire 3 mm region along with sections at 2 and 1.3 mm [9]. The derived rotational temperature was 150 K, and is fairly common not only for saturated cyanides, but also for the warmer parts of such hot cores. The attempts to identify *iso*-propyl cyanide in that molecular line survey of Sgr B2(N) were not conclusive and will be discussed with searches for other, related molecules in detail elsewhere. Further searches, in other sources or other frequency regions, can now be performed. The Boltzmann peak in the rotational spectrum of *iso*-propyl cyanide at 150 K occurs at 230 GHz. The strongest transitions in the 3 mm region are only about a factor of three weaker than those around the Boltzmann peak. Modeling of the data obtained in that line survey suggest that molecules as large as aminoacetonitrile [8], ethyl formate, or *n*-propyl cyanide [9] and with similar line intensities can be detected best in or near the 3 mm region in the case of observations with a single dish radio-telescope and if only

the rotational spectrum is considered. The single most important reason for this limitation is the plethora of spectral features caused by many small to medium sized molecules with fairly high abundances. Molecules with stronger lines, because of larger abundance, dipole moment, or rotational constants, may be detectable more favorably at frequencies closer to or even beyond the Boltzmann peak. For searches for molecules with weaker lines, lower frequencies are recommended. Resorting to array instruments, such as the Atacama Large Millimeter Array (ALMA) may well reduce the problem of line confusion, but the exact extent remains to be explored. At the upper frequency end of the present investigations, the intensities of the strongest lines at 150 K have dropped already by a factor of 40 from those at the Boltzmann peak, suggesting that searches for this molecule at such high frequencies are not reasonable. But even if ALMA should reveal even denser and hotter parts of the ISM in which molecules such as *iso*-propyl cyanide or complex ones may be detected, it should be kept in mind that extrapolations of the rotational spectrum should be reasonable up to about twice the upper frequency, which is well beyond the final ALMA range.

Besides rotational and centrifugal distortion parameters, greatly improved ^{14}N nuclear quadrupole coupling parameters as well as approximate values for the nuclear magnetic spin-rotation parameters have been obtained. Aided by quantum-chemical calculations, it was shown that the quadrupole tensor in its principal axis system is essentially identical to that of, e.g., methyl cyanide, as one would expect and as has been assumed previously.

An earlier value for the dipole moment component along the a -axis was confirmed and improved, and the value for the c -axis was revised downward considerably.

Acknowledgements

We appreciate the help of Frank Lewen and Christian P. Endres with the spectrometer systems. H.S.P.M. is very grateful to the Bundesministerium für Bildung und Forschung (BMBF) for financial support aimed at maintaining the Cologne Database for Molecular Spectroscopy, CDMS. This support has been administered by the Deutsches Zentrum für Luft- und Raumfahrt (DLR). A.C. and A.W. thank the French National Program PCMI (CNRS/INSU) and the Observatoire Midi-Pyrénées for funding. J.-U.G. acknowledges support by the Deutsche Forschungsgemeinschaft (DFG) and the Land Niedersachsen.

References

- [1] H.S.P. Müller, S. Thorwirth, D.A. Roth, G. Winnewisser, *Astron. Astrophys.* 370 (2001) L49–L52.
- [2] H.S.P. Müller, F. Schlöder, J. Stutzki, G. Winnewisser, *J. Mol. Struct.* 742 (2005) 215–227.
- [3] P.M. Solomon, K.B. Jefferts, A.A. Penzias, R.W. Wilson, *Astrophys. J.* 168 (1971) L107–L110.
- [4] M. Gerin, F. Combes, G. Wlodarczak, T. Jacq, M. Guélin, P. Encrenaz, C. Laurent, *Astron. Astrophys.* 259 (1992) L35–L38.
- [5] D.R. Johnson, F.J. Lovas, C.A. Gottlieb, E.W. Gottlieb, M.M. Litvak, M. Guélin, P. Thaddeus, *Astrophys. J.* 218 (1977) 370–376.
- [6] K. Demyk, H. Mäder, B. Tercero, J. Cernicharo, J. Demaison, L. Margulès, M. Wegner, S. Keipert, M. Sheng, *Astron. Astrophys.* 466 (2007) 255–259.
- [7] H.S.P. Müller, A. Belloche, K.M. Menten, C. Comito, P. Schilke, *J. Mol. Spectrosc.* 251 (2008) 319–325.
- [8] A. Belloche, K.M. Menten, C. Comito, H.S.P. Müller, P. Schilke, J. Ott, S. Thorwirth, C. Hieret, *Astron. Astrophys.* 482 (2008) 179–196.
- [9] A. Belloche, R.T. Garrod, H.S.P. Müller, K.M. Menten, C. Comito, P. Schilke, *Astron. Astrophys.* 499 (2009) 215–232.
- [10] G.E. Herberich, *Z. Naturforsch.* 22a (1967) 543–545.
- [11] J.R. Durig, Y.S. Li, *J. Mol. Struct.* 21 (1974) 289–297.
- [12] C.P. Endres, F. Lewen, T.F. Giesen, S. Schlemmer, D.G. Paveliev, Y.I. Koschurinov, V.M. Ustinov, A.E. Zhucov, *Rev. Sci. Instr.* 78 (2007) Art.-No. 043106.
- [13] G. Winnewisser, A.F. Krupnov, M.Y. Tret'yakov, M. Liedtke, F. Lewen, A.H. Saleck, R. Schieder, A.P. Shkarev, S.V. Volokhov, *J. Mol. Spectrosc.* 165 (1994) 294–300.
- [14] T.J. Balle, W.H. Flygare, *Rev. Sci. Instr.* 52 (1981) 33–45.
- [15] J.-U. Grabow, W. Stahl, *Z. Naturforsch.* 45a (1990) 1043–1044.
- [16] J.-U. Grabow, W. Stahl, *H. Dreizler Rev. Sci. Instr.* 67 (1996) 4072–4084.
- [17] J.-U. Grabow, E.S. Palmer, M.C. McCarthy, P. Thaddeus, *Rev. Sci. Instr.* 76 (2005) Art.-No. 093106.
- [18] M. Schnell, D. Banser, J.-U. Grabow, *Rev. Sci. Instr.* 75 (2004) 2111–2115.
- [19] Gaussian 03, Revision C.02, M.J. Frisch, G.W. Trucks, H.B. Schlegel, G.E. Scuseria, M.A. Robb, J.R. Cheeseman, J.A. Montgomery, Jr., T. Vreven, K.N. Kudin, J.C. Burant, J.M. Millam, S.S. Iyengar, J. Tomasi, V. Barone, B. Mennucci, M. Cossi, G. Scalmani, N. Rega, G.A. Petersson, H. Nakatsuji, M. Hada, M. Ehara, K. Toyota, R. Fukuda, J. Hasegawa, M. Ishida, T. Nakajima, Y. Honda, O. Kitao, H. Nakai, M. Klene, X. Li, J. E. Knox, H.P. Hratchian, J.B. Cross, C. Adamo, J. Jaramillo, R. Gomperts, R.E. Stratmann, O. Yazyev, A.J. Austin, R. Cammi, C. Pomelli, J.W. Ochterski, P.Y. Ayala, K. Morokuma, G.A. Voth, P. Salvador, J.J. Dannenberg, V.G. Zakrzewski, S. Dapprich, A.D. Daniels, M. C. Strain, O. Farkas, D.K. Malick, A.D. Rabuck, K. Raghavachari, J.B. Foresman, J.V. Ortiz, Q. Cui, A. G. Baboul, S. Clifford, J. Cioslowski, B.B. Stefanov, G. Liu, A. Liashenko, P. Piskorz, I. Komaromi, R.L. Martin, D.J. Fox, T. Keith, M.A. Al-Laham, C.Y. Peng, A. Nanayakkara, M. Challacombe, P.M.W. Gill, B. Johnson, W. Chen, M.W. Wong, C. Gonzalez, J.A. Pople, Gaussian, Inc., Wallingford CT, 2004.
- [20] K.A. Peterson, T.H. Dunning, *J. Chem. Phys.* 117 (2002) 10548–10560.
- [21] H.M. Pickett, *J. Mol. Spectrosc.* 148 (1991) 371–377.
- [22] F. Filsinger, K. Wohlfahrt, M. Schnell, J.-U. Grabow, J. Küpper, *Phys. Chem. Chem. Phys.* 10 (2008) 666–673.
- [23] K. Tanaka, T. Tanaka, I. Suzuki, *J. Chem. Phys.* 82 (1985) 2835–2844.
- [24] Z. Kisiel, J. Kosarzewski, B.A. Pietrewicz, L. Pszczółkowski, *Chem. Phys. Lett.* 325 (2000) 523–530.
- [25] G. Wlodarczak, L. Martinache, J. Demaison, K.-M. Marstokk, H. Möllendal, *J. Mol. Spectrosc.* 127 (1988) 178–185.
- [26] L. Bizzocchi, C. Degli Esposti, L. Dore, Z. Kisiel, *J. Mol. Spectrosc.* 251 (2008) 138–144.
- [27] H.S.P. Müller, G.O. Sørensen, M. Birk, R.R. Friedl, *J. Mol. Spectrosc.* 186 (1997) 177–188.
- [28] H. Spahn, H.S.P. Müller, T.F. Giesen, J.-U. Grabow, M.E. Harding, J. Gauss, *Chem. Phys.* 346 (2008) 132–138.
- [29] F.F.S. van der Tak, H.S.P. Müller, M.E. Harding, J. Gauss, *Astron. Astrophys.* 509 (2009) 347–354.
- [30] C. Puzzarini, G. Cazzoli, M.E. Harding, J. Vázquez, J. Gauss, *J. Chem. Phys.* 131 (2009) Art.-No. 234304.
- [31] G. Cazzoli, L. Dore, C. Puzzarini, J. Gauss, *Mol. Phys.* 108 (2010) 2335–2342.
- [32] H.S.P. Müller, M.C.L. Gerry, *J. Chem. Soc. Faraday Trans.* 90 (1994) 3473–3481.
- [33] K. Vormann, H. Dreizler, *Z. Naturforsch.* 43a (1988) 338–344.
- [34] Y.S. Li, M.D. Harmony, *J. Chem. Phys.* 50 (1969) 3674–3677.
- [35] G. Cazzoli, C. Puzzarini, *J. Mol. Spectrosc.* 240 (2006) 153–163.
- [36] H.S.P. Müller, B. J. Drouin, J. C. Pearson, *Astron. Astrophys.* 506 (2009) 1487–1499.
- [37] M. Stolze, D.H. Sutter, *Z. Naturforsch.* 40a (1985) 998–1010.
- [38] J.M. Colmont, G. Wlodarczak, D. Priem, H.S.P. Müller, E.H. Tien, R.J. Richards, M.C.L. Gerry, *J. Mol. Spectrosc.* 181 (1997) 330–344.

- [39] K. Wohlfahrt, M. Schnell, J.-U. Grabow, J. Küpper, *J. Mol. Spectrosc.* 247 (2008) 119–121.
- [40] R.L. DeLeon, J.S. Muentert, *J. Chem. Phys.* 82 (1985) 1702–1704.
- [41] M. Hahn, H.-K. Bodenseh, M. Ferner, *J. Mol. Spectrosc.* 223 (2004) 138–147.
- [42] M.C. McCarthy, J.-U. Grabow, M.J. Travers, W. Chen, C.A. Gottlieb, P. Thaddeus, *Astrophys. J.* 513 (1999) 305–310.
- [43] W.L. Ebenstein, J.S. Muentert, *J. Chem. Phys.* 80 (1984) 3989–3991.
- [44] A. Kraśnicki, L. Pszczółkowski, Z. Kisiel, *J. Mol. Spectrosc.* 260 (2010) 57–67.
- [45] R.K. Bohn, J.C. Pardus, J. August, T. Brupbacher, W. Jäger, *J. Mol. Struct.* 413–414 (1997) 293–300.
- [46] S.M. Fortman, I.R. Medvedev, C.F. Neese, F.C. De Lucia *Astrophys. J.* 714 (2010) 476–486.
- [47] J. Gadhi, A. Lahrouni, J. Legrand, J. Demaison, *J. Chim. Phys.* 92 (1995) 1984–1992.